SUPPLEMENTARY INFORMATION

Small molecule screening to reveal mechanisms underlying aquaporin-2 trafficking

Jana Bogum[1,2,3], Dörte Faust[1], Kerstin Zühlke[1,2], Jenny Eichhorst[2], Marie C. Moutty[1,2], Jens Furkert[2], Adeeb Eldahshan[1], Martin Neuenschwander[2], Jens Peter von Kries[2], Burkhard Wiesner[2], Christiane Trimpert[4], Peter M.T. Deen[4], Giovanna Valenti[5], Walter Rosenthal[1,6] and Enno Klussmann[1]

[1]Max Delbrueck Center for Molecular Medicine (MDC) Berlin, Germany

[2]Leibniz-Institut für Molekulare Pharmakologie (FMP), Berlin, Germany

[3]Department of Biology, Chemistry and Pharmacy, Freie Universität Berlin, Germany

[4]Department of Physiology, RUNMC Nijmegen, Radboud University Nijmegen Medical Centre, Nijmegen, The Netherlands

[5]Department of General and Environmental Physiology, University of Bari, Italy

[6]Charité University Medicine Berlin, Germany

Running title: Small molecules affecting AQP2

Corresponding author

Dr. Enno Klussmann

Max Delbrueck Center for Molecular Medicine (MDC), Berlin, Germany

Robert-Rössle-Str. 10

D-13125 Berlin

Tel. +49-(0)30-9406 2596

FAX. +49-(0)30-9406 2593

E-mail: enno.klussmann@mdc-berlin.de

Suppl. Fig.1

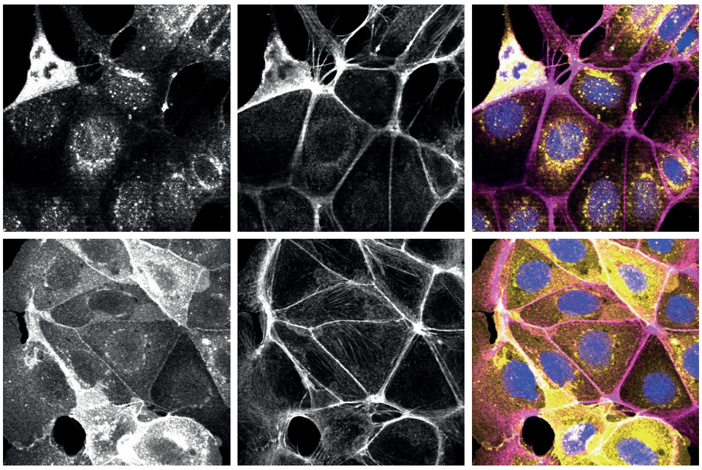

Detection of AQP2 and F-actin in mouse collecting duct cells stably expressing human AQP2 (MCD4 cells). MCD4 cells were treated with forskolin (FSK 10 µM, 20 minutes) or left untreated. Cells were fixed with paraformaldehyde, permeablized with Triton X-100 and AQP2 was detected by immunofluorescence microscopy with specific antibody H27 (Maric et al. AJP, 1998) and Cy3-coupled anti-rabbit secondary antibodies (yellow). F-actin was detected by TRITC-Phalloidin staining (magenta). Nuclei were stained with DAPI (blue). Fluorescence signals were visualized using a laser-scanning microscope (LSM 510 META, 100x magnification). Shown are representative images from three independent experiments.

Suppl. Fig. 2

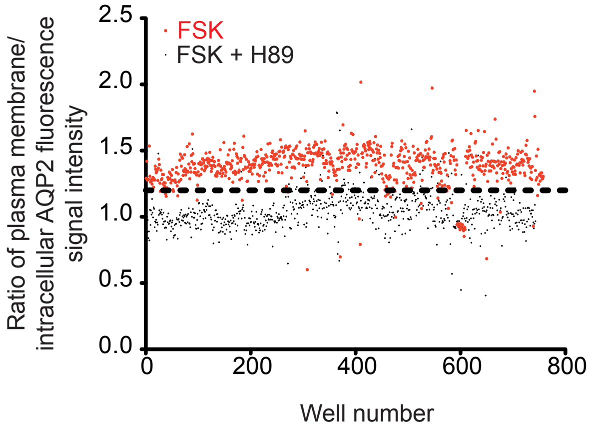

The localization of AQP2 in MCD4 cells in the presence of forskolin (FSK) or the combination of FSK and the PKA inhibitor H89. Primary screening was carried out in 384 well plates of MCD4 cells with 32 wells of controls in each plate, 16 wells treated with FSK alone (10 µM, 20 min) and 16 wells treated with a combination of FSK and H89 (30 µM, 100 min; see also Figs. 1A and B). The localization of AQP2 was expressed as ratio of fluorescence signal intensities at the plasma membrane to intracellular fluorescence signal intensity. The ratio determined in cells treated with FSK = 1.40 ± 0.1, for cells treated with the combination of FSK and H89 it was 0.91 ± 0.1. Based on these values, ratios ≤ 1.2 were considered low plasma membrane abundance (dashed line). Treatment of MCD4 cells with forskolin in the presence of 83 of the library compounds resulted in ratios ≤ 1.2, indicating that they inhibited the FSK-induced AQP2 redistribution (see Suppl. Tab. 1).

Suppl. Fig. 3

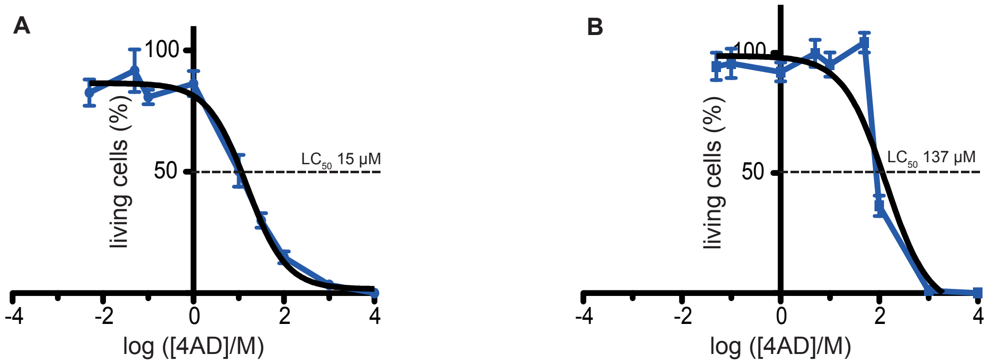

Determination of LC_{50} values for 4AD in MCD4 and IMCD cells. Cytotoxicity was evaluated using the MTT ((3-(4,5-Dimethylthiazol-2-yl)-2,5-diphenyltetrazolium bromide) assay. MCD4 (A) or primary IMCD cells (B) were seeded into 96 well plates, grown for 24 hours and left either untreated or incubated with 4AD in concentrations of 1 mM, 100, 50, 10, 1, 0.1, 0.05 and 0.05 µM for 24 hours. The 4AD-containing incubation medium was replaced by a solution of MTT in medium (0.5 mg/ml) followed by additional 4 hours of incubation. Metabolically active living cells reduce yellow water-soluble tetrazolium salt to violet water-insoluble formazan crystals. MTT solution was removed and cells were lysed with a mixture of DMSO, SDS and acetic acid (14.9 ml, 1.5g, 90µl) to dissolve formazan crystals. Absorbance at 595 nm wavelengths was determined using an EnSpire plate reader (PerkinElmer Inc., Rodgau, Germany). Values from untreated cells were referred to as 100 % vitality. Shown are averages from three independent experiments (mean ± SEM, quadruplicates per condition). LC50 values of 15 µM and 137 µM were determined for MCD4 and primary IMCD cells, respectively (Suppl. Fig. 2A and 2B). The reason for the 10fold difference is unclear. IMCD cells seem generally less susceptible for uptake of exogenous molecules than other cell types. For example, inhibition of Rho family members with bacterial toxins such as toxin B requires also 10fold higher concentrations than used for other cell types (Klussmann, E, Tamma, G, Lorenz, D, Wiesner, B, Maric, K, Hofmann, F, Aktories, K, Valenti, G, Rosenthal, W: An inhibitory role of Rho in the vasopressin-mediated translocation of aquaporin-2 into cell membranes of renal principal cells. The Journal of biological chemistry, 276: 20451-20457, 2001).

Suppl. Tab. 1

ID	structure and formula	ratio	plate	well	MW	logP	H-Acc.	H-Don.
201196	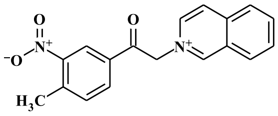 $C_{18}H_{15}N_2O_3$	0.23	72	G14	307.3	-0.51	3	0
214625	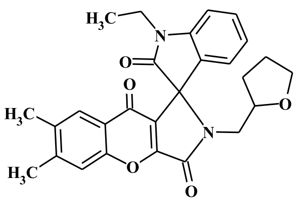 $C_{27}H_{26}N_2O_5$	0.54	110	B5	458.5	3.19	5	0
212086	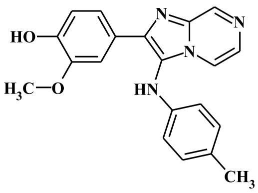 $C_{20}H_{18}N_4O_2$	0.57	103	K8	346.4	3.16	6	2
214590	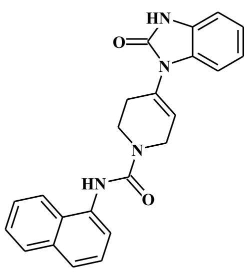 $C_{23}H_{20}N_4O_2$	*0.69*	*110*	*K18*	*384.4*	*3.24*	*2*	*2*
205831	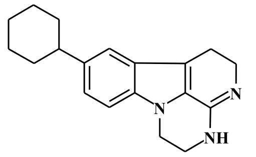 $C_{19}H_{23}N_3$	0.75	85	N5	293.4	3.62	2	1
214775	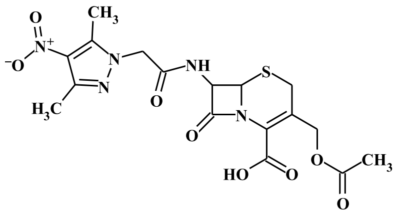 $C_{17}H_{19}N_5O_8S$	0.76	110	N20	453.4	-1.36	8	2
205653	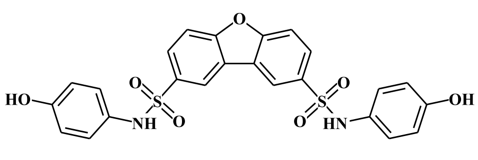 $C_{24}H_{18}N_2O_7S_2$	*0.78*	*85*	*I5*	*510.5*	*3.52*	*6*	*4*

214336	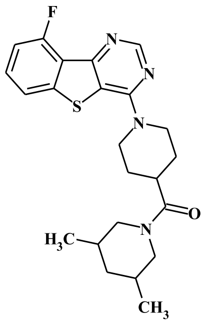 $C_{23}H_{27}FN_4OS$	0.79	109	P19	426.6	4.55	4	0
216086	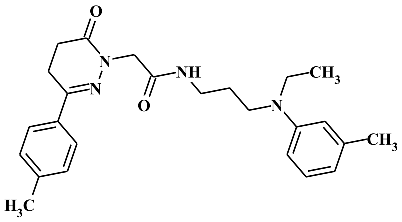 $C_{25}H_{32}N_4O_2$	*0.79*	*114*	*L17*	*420.5*	*3.47*	*4*	*1*
214645	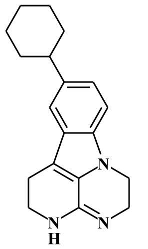 $C_{19}H_{23}N_3$	*0.8*	*110*	*J9*	*293.4*	*3.62*	*2*	*1*
200277	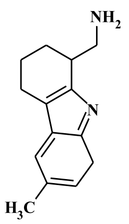 $C_{14}H_{18}N_2$	0.83	69	J4	214.31	1.22	2	1
205839	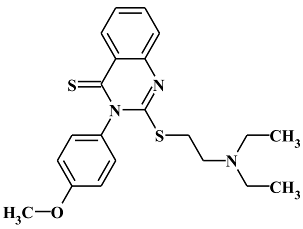 $C_{21}H_{25}N_3OS_2$	0.83	85	N7	399.6	5.23	3	0
206893	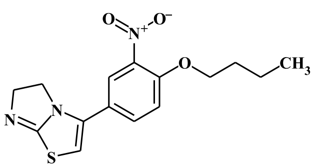 $C_{15}H_{17}N_3O_3S$	0.83	88	J7	319.4	3.07	5	0
216478	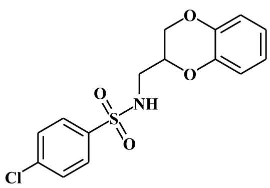 $C_{15}H_{14}ClNO_4S$	0.83	115	L6	339.8	2.78	4	1

205791	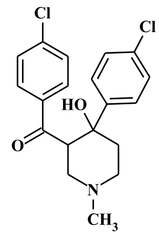 $C_{19}H_{19}Cl_2NO_2$	0.84	85	M18	364.3	3.73	3	1
212678	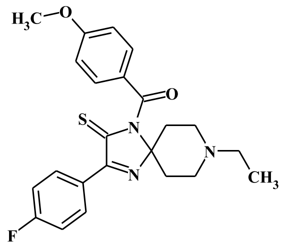 $C_{23}H_{24}FN_3O_2S$	***0.84***	***105***	***K1***	***425.5***	***4.99***	***4***	***0***
200728	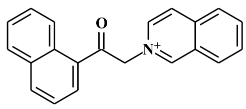 $C_{21}H_{16}NO$	0.86	71	O5	298.4	0.02	1	0
202659	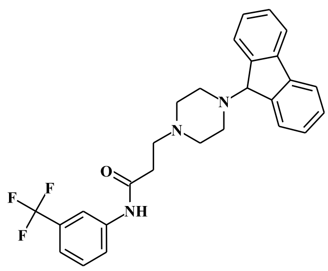 $C_{27}H_{26}F_3N_3O$	0.86	76	F5	465.5	5.25	3	1
215591	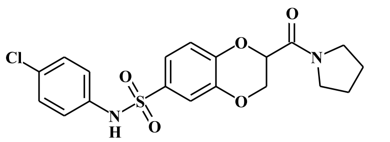 $C_{19}H_{19}ClN_2O_5S$	0.86	113	M4	422.9	2.31	5	1
200014	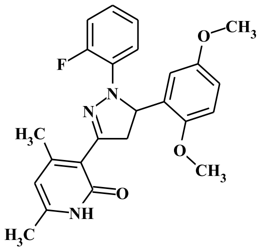 $C_{24}H_{24}FN_3O_3$	0.88	69	K3	421.5	4.09	5	1
212634	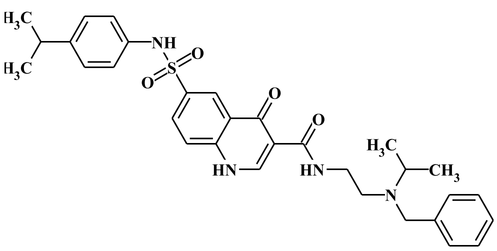 $C_{31}H_{36}N_4O_4S$	***0.88***	***104***	***D14***	***560.7***	***5.2***	***6***	***3***

4-acetydiphillin (4AD) 216407	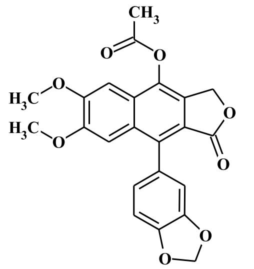 $C_{23}H_{18}O_8$	***0.88***	***115***	***N9***	***422.4***	***3.08***	***6***	***0***
203240	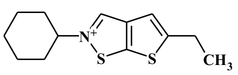 $C_{13}H_{18}NS_2$	*0.89*	*78*	*O17*	*252.4*	*1.6*	*0*	*0*
202254	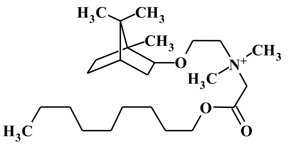 $C_{25}H_{48}NO_3$	0.9	75	K14	410.7	1.66	2	0
212248	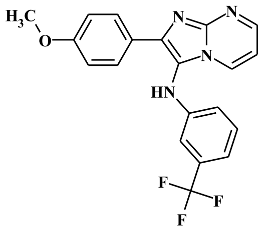 $C_{20}H_{15}F_3N_4O$	0.9	103	P4	384.4	4.09	5	1
215223	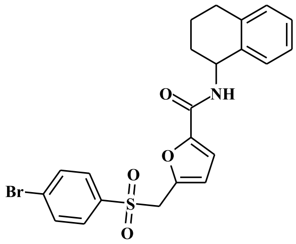 $C_{22}H_{20}BrNO_4S$	*0.9*	*112*	*M21*	*474.4*	*4.23*	*3*	*1*
216332	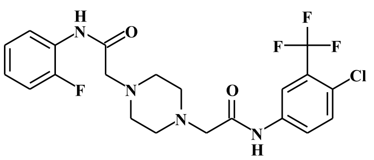 $C_{21}H_{21}ClF_4N_4O_2$	0.91	115	G14	472.9	2.84	4	2
100358	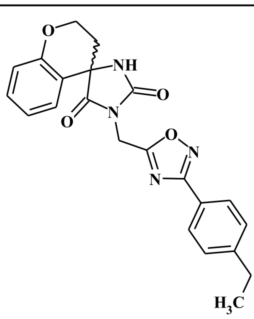 $C_{22}H_{20}N_4O_4$	0.91	1002	K1	404.4	3.46	5	1
208264	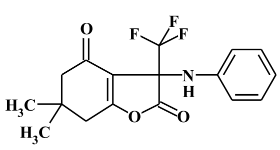 $C_{17}H_{16}F_3NO_3$	0.92	92	O20	339.3	3.18	3	1

202103	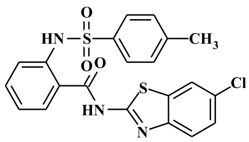 $C_{21}H_{16}ClN_3O_3S_2$	0.94	74	N20	457.9	5.49	4	2
201714	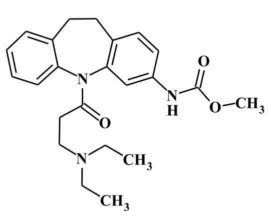 $C_{23}H_{29}N_3O_3$	0.95	73	D12	395.5	4	4	1
215677	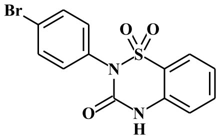 $C_{13}H_9BrN_2O_3S$	0.95	113	J3	353.2	3.51	3	1
209119	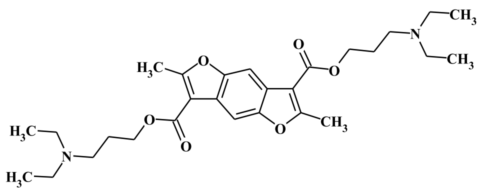 $C_{28}H_{40}N_2O_6$	0.97	94	N14	500.6	4.28	4	0
212576	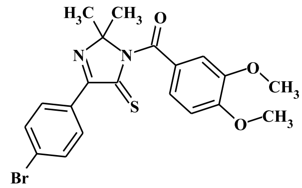 $C_{20}H_{19}BrN_2O_3S$	0.97	104	P19	447.3	4.75	4	0
207580	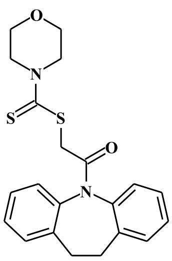 $C_{21}H_{22}N_2O_2S_2$	0.98	90	H3	398.5	4.15	2	0
208567	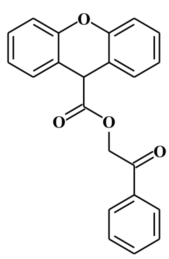 $C_{22}H_{16}O_4$	0.98	93	M8	344.4	4.19	2	0
216436	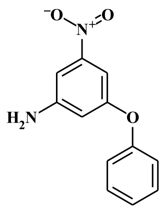 $C_{12}H_{10}N_2O_3$	0.98	115	H17	230.2	2.58	3	1

200360	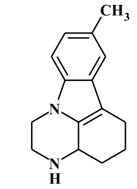 $C_{15}H_{18}N_2$	0.99	70	O1	226.3	3.1	1	1
205261	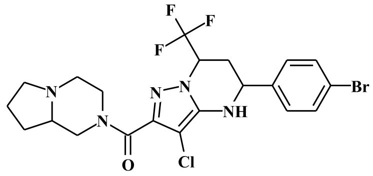 $C_{21}H_{22}BrClF_3N_5O$	1	83	J18	532.8	4.02	4	1
208431	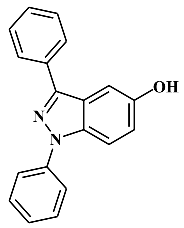 $C_{19}H_{14}N_2O$	1	92	N18	286.3	4.81	2	1
216542	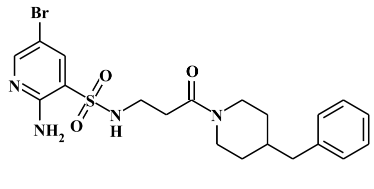 $C_{20}H_{25}BrN_4O_3S$	1	115	L22	481.4	2.19	5	2
100398	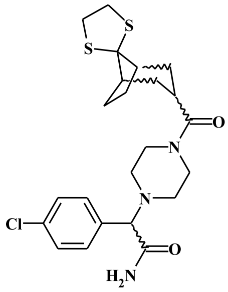 $C_{23}H_{30}ClN_3O_2S_2$	1	1002	K11	480.1	3.22	3	1
203313	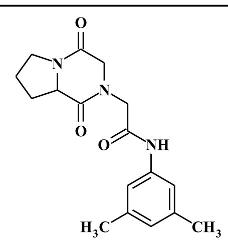 $C_{17}H_{21}N_3O_3$	*1*	*78*	*A16*	*315.4*	*0.79*	*3*	*1*
202336	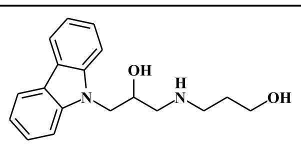 $C_{18}H_{22}N_2O_2$	***1***	***75***	***P11***	***298.4***	***1.69***	***3***	***3***
203067	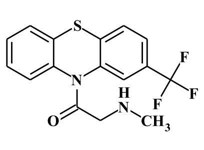 $C_{16}H_{13}F_3N_2OS$	1.01	77	F19	338.3	3.33	2	1

205221	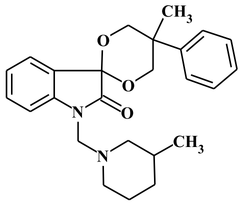 $C_{25}H_{30}N_2O_3$	1.01	83	J8	406.5	4.81	4	0
207724	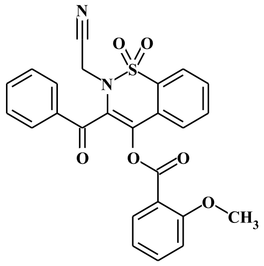 $C_{25}H_{18}N_2O_6S$	1.02	90	H18	474.5	3.27	6	0
201213	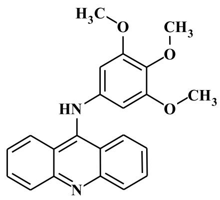 $C_{22}H_{20}N_2O_3$	*1.02*	*72*	*I18*	*360.4*	*4.47*	*5*	*1*
202806	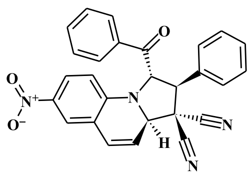 $C_{27}H_{18}N_4O_3$	1.03	76	L20	446.5	5.03	6	0
202886	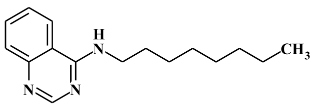 $C_{16}H_{23}N_3$	1.03	77	K17	257.4	4.59	3	1
205970	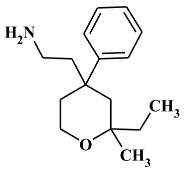 $C_{16}H_{25}NO$	1.03	85	D20	247.4	2.82	2	1
208599	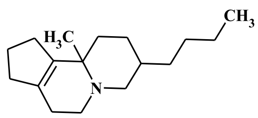 $C_{17}H_{29}N$	1.03	93	M16	247.4	4.19	1	0
205234	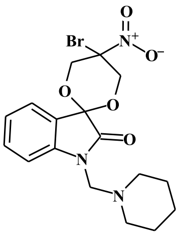 $C_{17}H_{20}BrN_3O_5$	1.04	83	D12	426.3	3.42	6	0

212622	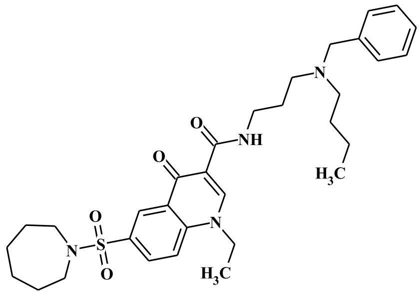 $C_{32}H_{44}N_4O_4S$	1.04	104	L10	580.8	4.62	6	1
200162	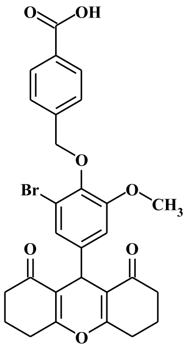 $C_{28}H_{25}BrO_7$	1.05	69	C20	553.4	4.56	7	1
202089	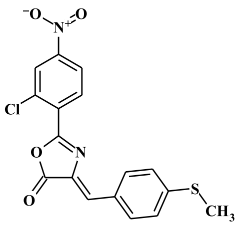 $C_{17}H_{11}ClN_2O_4S$	1.05	74	B18	374.8	5.01	4	0
205295	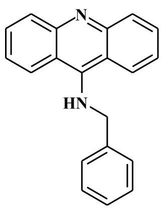 $C_{20}H_{16}N_2$	1.05	84	M3	284.4	4.7	2	1
208839	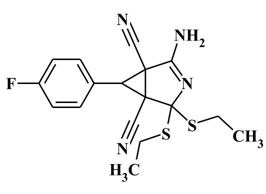 $C_{17}H_{17}FN_4S_2$	1.05	94	M9	360.5	3.11	4	1
209614	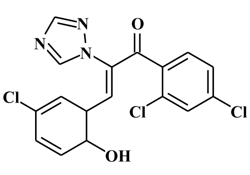 $C_{17}H_{10}Cl_3N_3O_2$	***1.06***	***96***	***K6***	***394.6***	***4.58***	***4***	***1***
205473	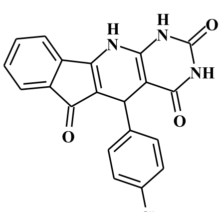 $C_{20}H_{12}ClN_3O_3$	1.07	84	B5	377.8	2.14	4	3

208677	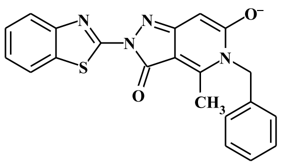 $C_{21}H_{15}N_4O_2S$	*1.07*	*93*	*J13*	*387.4*	*1.13*	*5*	*0*
200130	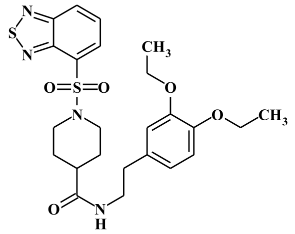 $C_{24}H_{30}N_4O_5S_2$	1.08	69	C12	518.6	3.07	7	1
205563	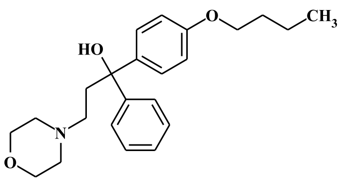 $C_{23}H_{31}NO_3$	1.08	84	F6	369.5	3.8	4	1
205343	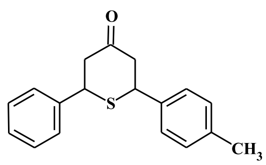 $C_{18}H_{18}OS$	1.09	84	M15	282.4	4.87	1	0
202554	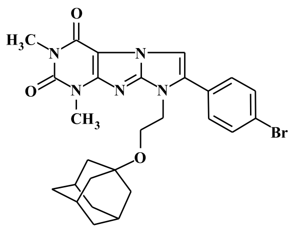 $C_{27}H_{30}BrN_5O_3$	1.12	76	C2	552.5	3.46	5	0
204317	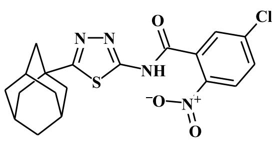 $C_{19}H_{19}ClN_4O_3S$	1.12	81	I2	418.9	4.79	5	1
202329	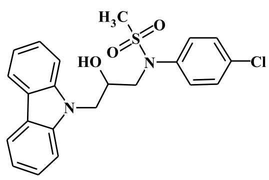 $C_{22}H_21ClN_2O_3S$	*1.12*	*75*	*B11*	*428.9*	*3.69*	*3*	*1*
204330	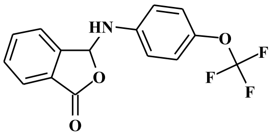 $C_{15}H_{10}F_3NO_3$	1.13	81	C6	309.2	4.56	3	1

205425	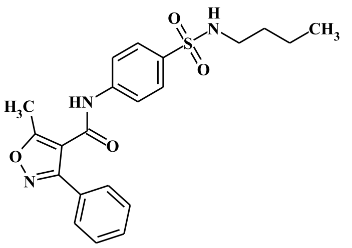 $C_{21}H_{23}N_3O_4S$	1.13	84	A16	413.5	3.82	4	2
202977	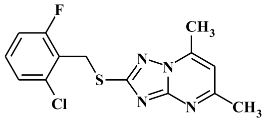 $C_{14}H_{12}ClFN_4S$	1.15	77	A20	322.8	4.22	4	0
204332	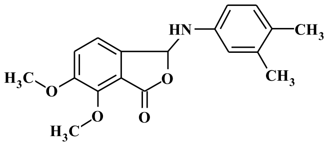 $C_{18}H_{19}NO_4$	*1.16*	*81*	*G6*	*313.3*	*3.84*	*4*	*1*
202747	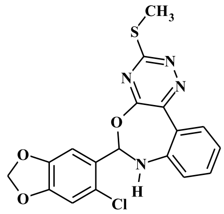 $C_{18}H_{13}ClN_4O_3S$	1.17	76	F6	400.8	4.43	7	1
201913	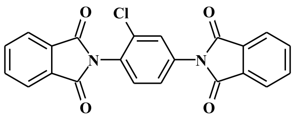 $C_{22}H_{11}ClN_2O_4$	1.18	74	A18	402.8	3.78	4	0
208469	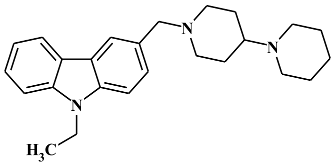 $C_{25}H_{33}N_3$	1.18	93	I5	375.5	4.49	2	0
209044	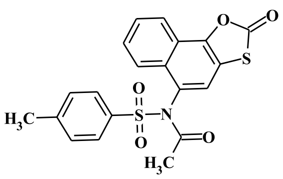 $C_{20}H_{15}NO_5S_2$	*1.18*	*94*	*H17*	*413.5*	*4.34*	*5*	*0*
201996	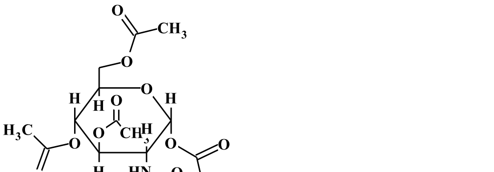 $C_{29}H_{49}NO_{10}$	1.19	74	H15	571.7	4.58	6	1
205599	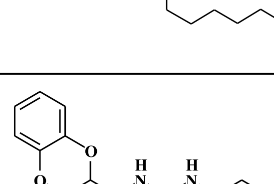 $C_{17}H_{18}N_2O_2S$	1.19	84	N14	314.4	3.78	2	2

205464	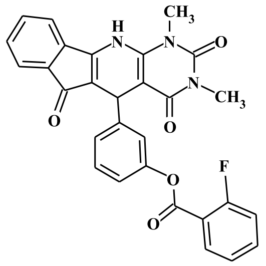 $C_{29}H_{20}FN_3O_5$	1.19	84	P1	509.5	3.78	5	1
202563	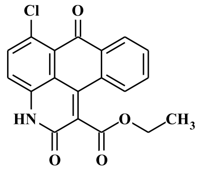 $C_{19}H_{12}ClNO_4$	1.2	76	E4	353.8	3.44	3	1
202803	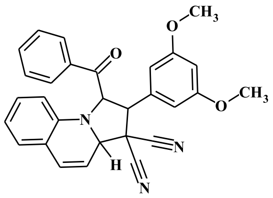 $C_{29}H_{23}N_3O_3$	1.2	76	F20	461.5	4.78	6	0
202733	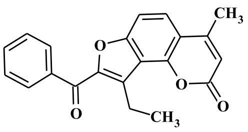 $C_{21}H_{16}O_4$	1.2	76	J2	332.3	4.58	2	0
203442	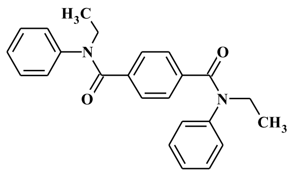 $C_{24}H_{24}N_2O_2$	1.2	78	D4	372.5	4.6	2	0
205444	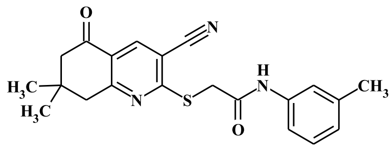 $C_{21}H_{21}N_3O_2S$	1.2	84	G20	379.5	3.72	4	1

Suppl. Tab. 1. Primary screening of 17,700 small molecules identified 83 inhibitors of the cAMP-induced redistribution of AQP2 in MCD4 cells. Compounds are ranked according to increasing ratios of plasma membrane/intracellular AQP2 fluorescence signal intensities. Compounds with ratios ≤ 1.2 were defined as inhibitory (a predominant intracellular localization of AQP2). Secondary screening revealed that 17 of the hits (italic) inhibited the AQP2 redistribution in MCD4 cells concentration-dependently. The inhibitory effect of 5 compounds (italic and bold) was also observed in IMCD cells. Compound ID numbers (ID), compound library positions (plate, well), molecular weight (MW), partition coefficient (logP), numbers of proton donor (H-Don.) and acceptor (H-Acc.) moieties are given for each substance.